INSTITUTE OF PHYSICS PUBLISHING SEMICONDUCTOR SCIENCE AND TECHNOLOGY
Semicond. Sci. Technol. **19** (2004) L69–L73 PII: S0268-1242(04)77286-7

LETTER TO THE EDITOR

Quantum transport under high-frequency conditions: application to bound state resonant tunnelling transistors

X Oriols[1], A Alarcón[1] and J Mateos[2]

[1] Department d'Enginyeria Electrònica, Universitat Autònoma de Barcelona, 08193 Bellaterra, Spain
[2] Departamento de Física Aplicada, Universidad de Salamanca, 37008 Salamanca, Spain

Received 4 March 2004
Published 18 May 2004
Online at stacks.iop.org/SST/19/L69
doi:10.1088/0268-1242/19/7/L01

Abstract
An approach for studying the performance of phase-coherent devices under high-frequency conditions is presented. The necessity of dealing with a scattering matrix that depends on the external frequency is emphasized, in order to provide an adequate theoretical framework for present tunnelling devices at frequencies comparable with the inverse of the electron transit time. As an example, a simple bound state resonant tunnelling transistor is studied. Its admittance parameters are computed showing that its amplifying properties are strongly degraded at THz frequencies. The present approach provides an original path for studying the ultimate quantum high-frequency limit for nanometric field effect transistors.

1. Introduction

The Landauer approach [1, 2] has become the fundamental framework for understanding most of the experiments in mesoscopic systems [3]. It is intuitively very appealing because it relates the macroscopic conductance of phase-coherent devices with the microscopic quantum mechanical (QM) transmission coefficient of electrons. However, the generalization of the Landauer approach to high-frequency alternating current (ac) conditions is far from trivial [2] because the modern QM approaches have to be compatible with the old electromagnetic theory. An important effort has been made by Buttiker and co-workers [4–6] to provide full quantum theories for phase-coherent devices under ac conditions. They succeeded in extending the Landauer approach to mesoscopic systems assuring overall current and charge conservation under ac conditions in the low-frequency limit, where any kinetic electron time associated with the device is much shorter than the reciprocal of the external ac frequency [6]. In this letter, we propose to overcome this limit by using a dynamic QM transmission coefficient for high-frequency ac conditions.

As an example, we study a bound state resonant tunnelling transistor (BSRTT) that is a typical double barrier-like heterostructure with a direct electric contact at the quantum well that works as a typical base electrode. This is achieved by converting the first resonance in the well (E_0) into a truly confined state by decreasing the band gap of the material in the quantum well (see scheme in figure 1). The second level (E_1) is then used for the standard resonant tunnelling transport between the emitter and the collector. Let us mention that although the BSRTT is very attractive from a theoretical point of view, and some prototypes have been already fabricated [7], a true contact of good quality on the quantum well (on such a thin layer) is very hard to achieve. From a technological point of view, three-terminal resonant tunnelling devices manipulating the peak current by means of Schottky gate [8, 9] are preferred. In any case, according to the goal of the present letter, the use of an ideal BSRTT provides an excellent opportunity for discussing the high-frequency quantum transport approach. For dc conditions, the static emitter–collector current, I_{dc}, through the BSRTT is computed

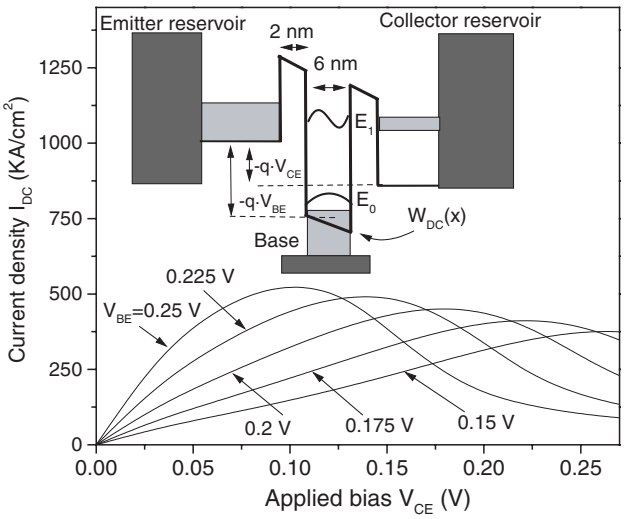

Figure 1. Amplifying characteristic of a typical BSRTT. Emitter–collector current, I_{dc}, as a function of the collector–emitter voltage, V_{ce}, for different applied voltages at the base contact $0.15\ V \leqslant V_{BE} \leqslant 0.25\ V$.

from the well-known Esaki formula [10, 11]:

$$I_{dc} = A\frac{qm}{\hbar^3}\frac{k_B\Theta}{2\pi^2} \times \int_{E=0}^{E=\infty} dE\, T_{dc}(E) \ln\left\{\frac{1+\exp((E_{fe}-E)/k_B\Theta)}{1+\exp((E_{fc}-E)/k_B\Theta)}\right\} \quad (1)$$

where q is the absolute electron charge, m is the GaAs effective mass equal to 0.067 times the free electron mass, $k_B\Theta$ is the thermal energy, A is the transversal area of the device and E_{fe}/E_{fc} are the emitter–collector Fermi levels. On the other hand, $T_{dc}(E)$ is the standard transmission coefficient computed from the solution of the Schrödinger equation under the static potential profile $W_{dc}(x)$ depicted in the scheme in figure 1.

The applied bias at the base contact, V_{BE}, determines the number of electrons in the bound state (E_0), and the depth of the quantum well. Therefore, the base contact effectively controls $T_{dc}(E)$ and I_{dc}, providing the typical transistor amplifying property. As a particular example, we consider two highly doped emitter–collector GaAs regions ($N_d = 1.5 \times 10^{18}$ cm^{-3}), two AlGaAs 0.3 eV height barriers of 2 nm and a 6 nm quantum well with a -0.2 eV band discontinuity with respect to the emitter–collector flat band conditions (see the scheme of figure 1). The typical current–voltage characteristic of the BSRTT is computed from equation (1) at 300 K with $E_{fe} = 0.05$ eV and $E_{fc} = E_{fe} - V_{CE}$. The device transconductance, at $V_{BE} = 0.2$ V and $V_{CE} = 0.1$ V, is around the value $g_{mo} = 10$ mS (4.27×10^{10} S m^{-2}) for a typical lateral area $A = 0.5 \times 0.5\ \mu$m^2.

2. Dynamic transmission coefficient

Our goal is to provide a discussion of the degradation of the amplifying properties of BSRTT when the inverse of the electron transit time is comparable with the external ac frequency. As discussed in the introduction, most QM

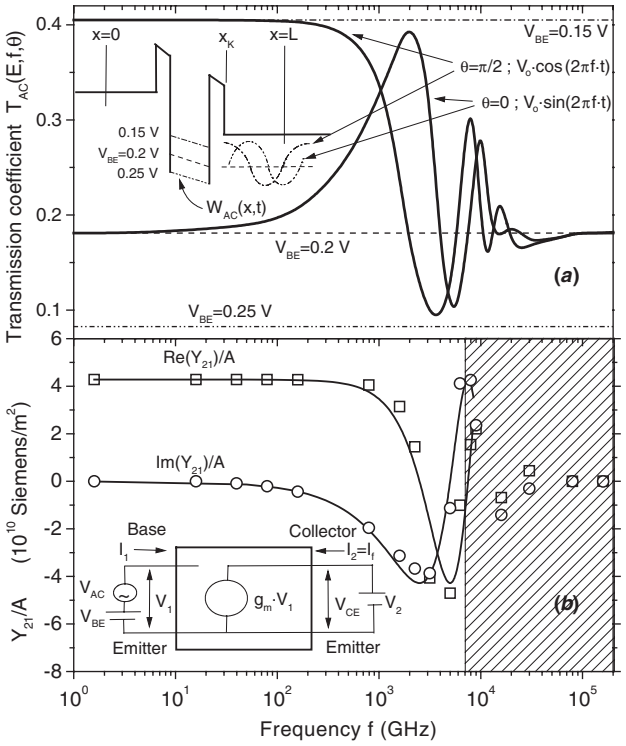

Figure 2. (*a*) Solid line: $T_{ac}(E, f, \theta)$ for an electron with central energy 0.15 eV impinging upon two different (cosine $\theta = \pi/2$ and sine $\theta = 0$) oscillating potential profiles depicted in the scheme. Horizontal dashed lines correspond to $T_{dc}(E)$ for $V_{BE} = 0.15$ V (dash-dot line), $V_{BE} = 0.20$ V (dash line) and $V_{BE} = 0.25$ V (dash-dot-dot line); (*b*) symbols: the complex small-signal admittance parameter Y_{21} for the BSRTT; solid line: the Y-parameter approximation (retarded transfer function) $Y_{21}(f) = g_{mo}\exp(-j2\pi f\tau)$ [15]. The shaded region shows the microwave frequencies where the electromagnetic vector potential becomes meaningful (see footnote 4).

theories are based on a frequency-independent scattering matrix approach [6] (i.e. the QM transmission coefficient does not depend on the external frequency) that precludes the possibility of studying the ultimate cut-off frequency due to tunnelling. For dc conditions, tunnelling can be easily understood from the spatial phase coherence of the electrons (i.e. from the static potential profile $W_{dc}(x)$ along the device). However, when oscillating potentials are considered, tunnelling is due to the spatial and also to the temporal QM coherence of the electron.

In our approach, the time-dependent wave-like nature of electrons is described by wave packet, $\Psi(x, t)$, solutions of the Schrödinger equation under time-dependent Hamiltonians. Therefore, the *dynamic* transmission coefficient, $T_{ac}(E, f, \theta)$, is computed as the total probability, at the right of the barrier region (defined as $x > x_K$ in the scheme of figure 2(*a*)), evaluated when the electron interaction with the barriers is finished:

$$T_{ac}(E, f, \theta) = \int_{x=x_K}^{X=\infty} |\Psi(x, t \to \infty)|^2\, dx \equiv \int_{t=0}^{\infty} J(x_l, t)\, dt. \quad (2)$$

From the QM particle conservation law, we know that the number of particles transmitted through the barrier can also

be computed from the QM particle current density, $J(x_l, t)$, and this number is independent of the position, x_l, where the current is evaluated (equation (2)). Let us note that the time dependence of the Hamiltonian precludes the possibility of using standard diagonalized eigenstates. The crucial point of our approach is the fact that $T_{ac}(E, f, \theta)$ depends on the oscillating frequency f and the phase θ of the potential profile $W_{ac}(x, t)$. Such a potential, $W_{ac}(x, t)$, is defined as the flat dc profile[3], everywhere except in the quantum well where $W_{ac}(x, t) = W_{dc}(x) - qV_0 \sin(2\pi f t + \theta)$. We use $\theta_I = 0$ for the sinusoidal base signal and $\theta_R = \pi/2$ for the cosinusoidal base signal. The wavefunction at any time and position, $\Psi(x, t)$, is obtained by numerically solving (with a finite difference scheme) the Schrödinger equation under the previous time-dependent potential profile $W_{ac}(x, t)$. For practical proposals, the wavefunction is initially defined by a Gaussian wave packet located far from the barriers so that the probability presence inside the region $0 < x < L$ (as seen in the scheme in figure 2(*a*)) is negligible at $t = 0$.

In figure 2(*a*), we have represented $T_{ac}(E, f, \theta)$ for an initial Gaussian wave packet (with central energy $E = 0.15$ eV and spatial dispersion $\sigma = 10$ nm) impinging upon the previous BSRTT when a oscillating voltage is applied at the base contact with a small amplitude $V_0 = 0.05$ V around the dc bias $V_{BE} = 0.2$ V. As seen in figure 2(*a*), the *dynamic* transmission coefficient depends on frequency and also on the phase of the ac signal, but tends to the *static* value $T_{ac}(E, f, \theta)|_{f\to\infty} = T_{dc}(E)|_{V_{BE}=0.2\,V}$ for very high frequencies, independent of any ac parameter. Therefore, the amplifying ability of the BSRTT is ultimately limited due to the fact that QM tunnelling process can be slower than the oscillating signal applied to the base contact.

At this point, let us mention that identical physical results and explanations have been obtained within the Floquet theory [12, 13], where our *dynamic* transmission coefficient (equation (2)) is understood as a multiphoton scattering process that relates input and output energies of different Floquet states [13]. In any case, our approach can be generalized to any arbitrary dynamic Hamiltonian, and not only to the time-periodic ones [12]. Moreover, Floquet-based approaches are focused on time-averaged current under oscillating conditions. In section 4, we will use the *dynamic* transmission coefficient defined in equation (2) to compute the QM current under high-frequency conditions.

3. Small-signal transconductance

Now, let us note that any experimental characterization of electron devices above GHz frequencies is carried out via measurement of external *S*-parameters. Such parameters can be related to the intrinsic small-signal admittance matrix[4]. In the scheme of figure 2(*b*), we have represented the equivalent-circuit representation (*Y*-parameters) for a common-emitter configuration of the BSRTT interpreted as a two-port network (no capacitive effects are considered[5]). In order to compute the small-signal *Y*-parameters, we employ the sinusoidal steady-state analysis [14]. Thus, the input small-signal voltage applied at the base contact can be represented by a complex vector, $V_{ac}(t) = V_0 \exp(\mathrm{j}2\pi f t)$ (i.e. two different sinusoidal voltages dephased 90°). Then, the related output complex current has a real part, $I_R(t)$, and an imaginary part, $I_I(t)$, which can be computed as [15]:

$$\begin{aligned} I_R(t) - I_{dc} + \mathrm{j}(I_I(t) - I_{dc}) &= \Im\lfloor V_0 \exp(\mathrm{j}2\pi f t)\rfloor \\ &= V_0\,\Im[\cos(2\pi f t)] + \mathrm{j}V_0\,\Im[\sin(2\pi f t)] \end{aligned} \tag{3}$$

where $\Im$ is the linear system response that relates the input voltage to the output current. The value $I_{dc} = \Im[V_{BE}]$ is the output dc current without input small signal (equation (1)). Due to linearity, the real part of the output current is equal to the system response when the input small signal voltage is only $V_0 \cos(2\pi f t)$, and the imaginary part of the current is related only to $V_0 \sin(2\pi f t)$. Alternatively, the input/output relationships can be established in the frequency domain [15], via the steady-state (transfer function) transconductance $Y_{21}(f)$:

$$I_R(t) - I_{dc} + \mathrm{j}(I_I(t) - I_{dc}) = Y_{21}(f) V_0 \exp(\mathrm{j}2\pi f t). \tag{4}$$

Evaluating expression (4) at time $t = 0$, we obtain a useful expression for the complex transconductance:

$$\begin{aligned} \mathrm{Re}(Y_{21}(f)) &= \frac{I_R(t=0) - I_{dc}}{V_0} \\ \mathrm{Im}(Y_{21}(f)) &= \frac{I_I(t=0) - I_{dc}}{V_0}. \end{aligned} \tag{5}$$

Let us emphasize that the time when the current is evaluated, $t = 0$, has to be determined according to the phase of the input small-signal voltage. Moreover, at time $t = 0$, there are particles inside the device active region that still 'keep' information of the phase θ (sine or cosine) of the input signal.

4. Instantaneous current

In this section, we will use the time dependent wavefunction used for definition of *dynamic* transmission coefficient (anticipated in section 2) to provide an expression for the output current of tunnelling devices under ac conditions. After that, from the current, the complex high-frequency transconductance for mesoscopic systems is obtained using expression (5). In general, the instantaneous current can be computed at any time (in particular at $t = 0$) according to the extension of the Ramo–Shockley theorem to semiconductor devices [16],

$$I_{R/I}(t) = \frac{q}{L} \sum_{i=1}^{N(t)} v_i(x, t) \tag{6}$$

where L is the length of the active device region, $N(t)$ is the total number of carriers which are instantaneously inside the

[3] A high doping density ($N_d = 5 \times 10^{22}$ cm^{-3} for $E_f = 0.05$ eV) is used to assure a short screening length of the electric field at the emitter/collector regions.

[4] The use of standard circuit theory (i.e. the admittance parameters) is justified because it is well known that the role of the electromagnetic vector potential can be disregarded when the device size is much smaller than the minimum wavelength of the electromagnetic field (see [15]). For the lateral dimensions considered here (i.e. 0.5 μm), the electromagnetic vector potential can be disregarded for frequencies lower than 10 THz (see shaded picture in figure 2(*b*)).

[5] The build-up of charge and the associated time-dependent electric fields induce displacement currents along the system that have to be considered, in principle, to assure current continuity.

device, and $v_i(x,t)$ is the electron velocity. A monoenergetic beam of particles can be thought of as a constant flux of identical time-dependent wave packets, $\Psi(x,t)$, each one leaving the emitter reservoir and entering into the active device region at different times t_i. Therefore, at time $t=0$, each i-particle inside the device can also be levelled by its injecting time t_i (with $-\infty < t_i \leqslant 0$), and the wavefunction associated with this i-particle is $\Psi_i(x,t)$. Bearing in mind quantum trajectories described by the de Broglie–Bohm approach [17, 18], the instantaneous velocity for each i-particle is determined by the wavefunction [19]:

$$v_i(x,t) = \frac{J_i(x,t)}{|\Psi_i(x,t)|^2}. \tag{7}$$

Assuming a large number of particles (i.e. large lateral area $A = 0.5 \times 0.5\ \mu\text{m}^2$), then the sum over all particles in expression (6), at time $t=0$, can be related to a double integral over all injection times and positions inside the device $\sum_{i=1}^{N(t)} \rightarrow \int_{-\infty}^{0} \mathrm{d}t_i \int_0^L \mathrm{d}x |\Psi_i(x,0)|^2$. Using expressions (6) and (7), we conclude that the real/imaginary part of the output current can be computed at the initial time by

$$I_{\mathrm{R/I}}(t=0) = C\frac{q}{L}\int_{t_i=-\infty}^{0} \mathrm{d}t_i \int_{x=0}^{L} \mathrm{d}x\, J_i(x,0) \tag{8}$$

where we have to compute the QM particle current at $t=0$ for each injecting time. The effective electron injection rate for a monoenergetic flux of particles determines the value of the constant C as described in [19]. The generalization to all energies can be straightforwardly obtained by weighting each energy according to Fermi–Dirac statistics. Then, the total current $I_{\mathrm{R/I}}(t=0)$ is intuitively very appealing, since expression (1) is exactly recovered for static potentials.

Once the current is known, using expressions (5), we can compute the small-signal complex transconductance[6]. As anticipated, the descriptions of the current $I_{\mathrm{R/I}}(t=0)$ in phase-coherent systems (equation (8)) and of the complex transconductance (equation (5)) are the main results of the present letter.

5. Numerical results

Now, as an example, let us discuss the high-frequency transconductance of the BSRTT described in the introduction. In figure 2(b) we have represented Y_{21} as a function of the base-signal oscillating frequency for $V_{\mathrm{CE}} = 0.1$ V and $V_{\mathrm{BE}} = 0.2$ V. For low frequencies (i.e., when the electron transit time is much shorter than $1/f$) the phase of the ac voltage is almost zero for times of the order of the electron transit time (i.e., $V_0 \exp(\mathrm{j}2\pi f t) \approx V_0$), hence, the dc transconductance $g_{\mathrm{mo}} = 4.27 \times 10^{10}$ S m^{-2} is obtained. However, when the frequency increases above 100 GHz, the phase of the input small signal becomes meaningful for times of the order of the electron transit time and this fact largely affects the electron transmission probability (see figure 2(a)) and, as a direct consequence, $\mathrm{Re}(Y_{21})$ and $\mathrm{Im}(Y_{21})$ decrease[6] (see figure 2(b)). For very high frequency (much higher than the inverse of the electron transit time), the transmission coefficient is independent of any ac small-signal parameter, and the amplifying properties of the BSRTT completely disappear. From these results, we conclude that the performance of the BSRTT considered in this work is strongly degraded at frequencies of few THz due to the tunnelling process. As represented in the solid line of figure 2(b), the role of the electron QM tunnelling time on the high-frequency performance can be simply characterized by a retarded transfer function $Y_{21}(f) = g_{\mathrm{mo}} \exp(-\mathrm{j}2\pi f\tau)$ with $g_{\mathrm{mo}} = 4.27 \times 10^{10}$ S m^{-2} and $\tau = 0.1$ ps for a broad frequency spectrum[7].

Finally, let us make a comment on the range of validity of the present approach. It can be used for modelling nanometric field effect transistors, where two terminals are under dc conditions and the third one interacts with them via the electric field. It is assumed that global current and charge conservation are assured under the assumptions mentioned in footnotes 3, 4 and 5. In any case, for a general device, the implicit consideration of the capacitive effects (Coulomb interaction between electrons) will only contribute to a reduction of the intrinsic QM cut-off frequency obtained here. Therefore, the present THz limit cannot be overcome and has to be understood as a ultimate pure QM limitation due to the wave-like nature of electrons, which is much lower than the classical ballistic frequency limitation[8]. In addition, the intrinsic QM cut-off frequency provides an indirect measure of the electron transit time that opens a new path for studying the controversial issue of tunnelling times (experimental results for double barrier structures with barrier widths of 9 nm provide characteristic times of a few nanoseconds [20] and cut-off frequencies lower than 1 GHz, where the capacitive effects are negligible).

6. Conclusions

In conclusion, we have presented a suitable approach for studying the high-frequency performance of nanoscale devices under ac conditions (via a *dynamic* transmission coefficient). We have emphasized the necessity of dealing with a scattering matrix that depends on the external ac-oscillating frequency in order to study current nanoscale devices at GHz frequencies. The main results obtained in this letter are the description of the electron current $I_{\mathrm{R/I}}(t=0)$ under ac conditions for phase-coherent systems (equation (8)), and the evaluation of the complex transconductance (equation (5)). We have applied these results to study the high-frequency transconductance of a BSRTT with standard GaAs barrier (the approach can be generalized to any field effect transistor), and we have found out that quantum transport sets an intrinsic frequency limitation of few THz (the consideration of capacitive effects will only reduce the previously mentioned ultimate QM frequency limitation).

[6] The dynamic transmission coefficient (equation (2)) involves positive times ($0 \leqslant t < \infty$). However, the output current (equation (8)) involves negative times ($-\infty < t_i \leqslant 0$). Such a difference does not affect the transconductance when time-symmetrical, $W_{\mathrm{ac}}(x,-t) = W_{\mathrm{ac}}(x,t)$, potential profiles are considered. In contrast, the sign of $\mathrm{Im}(Y_{21})$ needs to be inverted since the sinusoidal potential profile is antisymmetrical with time, $W_{\mathrm{ac}}(x,-t) = -W_{\mathrm{ac}}(x,t)$.

[7] Transit time in tunnelling devices can also be heuristically obtained from the quasibound-state lifetime (i.e. the energy–time uncertainty). The tunnelling time obtained from the transmission spectrum of BSRTT is $\tau' = h/\Gamma \approx 0.14$ ps (where Γ is the full width at half maximum of the second transmission peak and h the Plank constant).

[8] Transit times for classical ballistic transport through the double barrier region $\tau'' = L/v = 0.01$ ps (for $L = 10$ nm and $v = 5 \times 10^5$ m s^{-1}) are much smaller than the QM values obtained with our approach.

Acknowledgments

The authors are really grateful to Olivier Vanbésien from IEMN (Institut d'Electronique, de Microélectronique et de Nanotechnologie), for reading the manuscript prior to its publication and to Eduard Fernández-Díaz for stimulating discussions. This work has been partially supported by the Ministerio de Ciencia y Tecnología and FEDER through projects TIC2003-08213-C02-02, TIC2001-1754 and by the Junta de Castilla y León through the project SA057/02.

References

[1] Landauer R 1970 Electrical resistance of disordered one-dimensional lattices *Phil. Mag.* **21** 863

[2] Landauer R 1992 Conductance from transmission: common sense points *Phys. Scr.* T **42** 110

[3] Datta S 1995 *Electronic Transport in Mesoscopic Systems* (Cambridge: Cambridge University Press)

[4] Büttiker M 1993 Capacitance, admittance, and rectification properties of small conductors *J. Phys.: Condens. Matter* **5** 9361

[5] Pretre A, Thomas H and Büttiker M 1996 Dynamic admittance of mesoscopic conductors: discrete-potential model *Phys. Rev.* B **54** 8130

[6] Blanter Y and Büttiker M 2000 Shot noise in mesoscopic conductors *Phys. Rep.* **336** 1

[7] Chen W L, Haddad G I, Munns G O and East J R 1993 Experimental realization of bound state resonant tunnelling transistor *IEEE Trans. Electron Devices* **40** 2133

[8] Peatman W C B, Brown E R, Rooks M J, Maki P, Grimm W J and Shur M 1994 Novel resonant tunnelling transistor with high transconductance at room temperature *IEEE Electron Device Lett.* **15** 236

[9] Ando Y and Cappy A 1998 Proposal of low-noise amplifier utilizing tunnelling transistors *IEEE Trans. Electron Devices* **45** 31

[10] Tsu R and Esaki L 1973 Tunnelling in a finite superlattice *Appl. Phys. Lett.* **22** 562

[11] Esaki L and Chang L L 1974 New transport phenomenon in a semiconductor superlattice *Phys. Rev. Lett.* **33** 495

[12] Grifoni M and Hanggi P 1998 Driven quantum tunnelling *Phys. Rep.* **304** 229

[13] Henseler M, Dittrich T and Richter K 2001 Classical and quantum periodically driven scattering in one dimension *Phys. Rev.* E **64** 046218

[14] Laux S 1985 Techniques for small-signal analysis of semiconductor devices *IEEE Trans. Electron Devices* **32** 2028

[15] Bruce-Carlson A 1986 *Communication Systems* (New York: McGarw-Hill)

[16] Pellegrini B 1986 Electric charge motion, induced current, energy balance, and noise *Phys. Rev.* B **34** 5921
Pellegrini B 1993 Extension of the electrokinematics theorem to the electromagnetic field and quantum mechanics *Nuovo Cimento* **14** 855

[17] Bohm D 1952 A suggested interpretation of the quantum theory in terms of hidden variables *Phys. Rev.* **85** 166
Holland P R 1993 *The Quantum Theory of Motion* (Cambridge: Cambridge University Press)

[18] Oriols X, Martín F and Suñé J 1996 Implications of the noncrossing property of Bohm trajectories in one-dimensional tunnelling configurations *Phys. Rev.* A **54** 2594

[19] Oriols X, Martín F and Suñé J 2001 Approach to study the noise properties in nanometric devices *Appl. Phys. Lett.* **79** 1703
Oriols X, Martín F and Suñé J 2002 High frequency components of current fluctuations in semiconductor tunnelling barriers *Appl. Phys. Lett.* **80** 4048

[20] Vanbésien O, Sadaune V, Lippens D, Vinter B, Bois P and Nagle J 1992 Direct evidences of the quasibound-state lifetime effect in resonant tunnelling from impedance measurements *Microw. Opt. Technol. Lett.* **5** 351